Precise ab initio calculations of ${}^{4}\text{He}(1snp\,{}^{3}P_{J})$ fine structure of high Rydberg states

Hao Fang¹,* Jing Chi^{1,2},* Xiao-Qiu Qi³, Yong-Hui Zhang¹,[†] Li-Yan Tang¹,[‡] and Ting-Yun Shi¹

¹Innovation Academy for Precision Measurement Science and Technology,

Chinese Academy of Sciences, Wuhan 430071, China

²University of Chinese Academy of Sciences, Beijing 100049, China and

³Department of Physics, Zhejiang Sci-Tech University, Hangzhou 310018, China

(Dated: November 3, 2025)

High-precision measurements of the fine-structure splittings in helium high Rydberg states have been reported, yet corresponding ab initio benchmarks for direct comparison remain unavailable. In this work, we extend the correlated B-spline basis function (C-BSBF) method to calculate the fine-structure splittings of high Rydberg states in $^4{\rm He}$. The calculations include the $m\alpha^4$ - and $m\alpha^5$ -order contributions, the singlet–triplet mixing effect, and estimated spin-dependent $m\alpha^6$ -order corrections obtained using a $1/n^3$ scaling approximation. High-precision ab initio results are obtained for principal quantum numbers n=24–37 with kilohertz-level accuracy and further extended to n=45–51 by extrapolation and fitting. The theoretical results show excellent agreement with quantum-defect theory (QDT) predictions and allow direct comparison with experimental measurements. Additionally, the discrepancy observed at n=34 is expected to be clarified with improved experimental precision.

PACS numbers: 31.30.J-, 31.15.-p, 31.15.ac

I. INTRODUCTION

The helium fine structure has attracted significant theoretical and experimental interest ever since Schwartz proposed the intervals of the $1s2p^3P_I$ states as a sensitive probe of the fine-structure constant α [1]. The $J=2\rightarrow 0$ interval has been measured with an accuracy of 130 Hz, which, if matched by complete $m\alpha^8$ -order QED calculations, could enable a determination of the fine-structure constant at the 2-ppb level [2]. Nevertheless, the required theoretical calculations appear to be too complicated to be accomplished in the near future [3]. For other two intervals of $J=2\to 1$ and $J=1\to 0$, the current measurements have achieved a precision on the order of tens of Hz [4, 5]. However, these results deviate from theoretical predictions [6] by 1.5 and 1.6 σ , respectively. Further advances in theoretical precision are mainly hindered by uncertainties in higher-order QED corrections [6, 7]. In addition, for the Rydberg fine-structure intervals with principle quantum numbers n below 10, high-precision calculations and measurements have been performed in order to test the long-range interactions between the Rydberg electron and the ionic core [8–11].

For higher values of n, measurements of the fine structure in helium are of great importance for various applications, including hybrid cavity quantum electrodynamics and quantum information processing [12, 13], as well as for studies of Förster resonance energy transfer in collisions with polar ground-state molecules [14]. Significant progress has been made in measuring the fine structures of these higher Rydberg states [15]. Using

microwave spectroscopy, Deller and Hogan observed the fine-structure intervals for n=34 to 36, and also resolved the large intervals of more highly excited states with n between 45 and 51, achieving transition-frequency uncertainties of 15–40 kHz [15]. Most of the measured intervals agreed well with the quantum defect results [16], but a significant discrepancy was found for n=34 [15]. Given that quantum defect theory (QDT) is not an exact fundamental theory [17], and that relativistic and QED corrections for higher Rydberg states scale as $1/n^3$, higher-order effects can be neglected. Consequently, high-precision ab initio calculations of the fine structures in helium Rydberg states are both practically feasible and theoretically essential.

Theoretically, benchmark ab initio data remain concentrated on low-lying states (roughly n < 10 with L < 7) [18–20] while analyses of higher n states typically rely on QDT, since conventional variational expansions rapidly lose accuracy with increasing n owing to the large radial-scale separation between the core and Rydberg electrons. Recently, by employing "triple" Hylleraas basis sets that simultaneously resolve short-range correlation and long-range Rydberg behavior, Bondy et al. [21] overcame this limitation and reported a kHz-level determination of the ionization energy for the $24^{1}P_{1}$ state. This pioneering high-accuracy ab initio calculation in the high-n regime demonstrated that a systematic extension of precision theoretical methods to Rydberg states is now feasible. The Rydberg states investigated experimentally [15, 22-24] typically lie at much higher principal quantum numbers. The above approach employing "triple" Hylleraas basis sets has only very recently enabled ab initio calculations to be extended to as high as n = 35 [25]; however, their work has mainly focused on the ionization energy.

In contrast to multiple-scale Hylleraas basis, we de-

^{*} These authors contributed equally to this work.

[†] yhzhang@wipm.ac.cn

[‡] lytang@apm.ac.cn

veloped the correlated B-spline basis-function (C-BSBF) method to enable high-precision calculations for both low-lying and Rydberg states of helium [26–29]. The C-BSBFs inherently accommodate the multiscale character of Rydberg helium. Accurate energies and polarizabilities have previously been reported for states up to n=10[26, 27, 29], and more recently, nonrelativistic energies of the Rydberg $1snp^{1,3}P$ states up to n=27 [30] were obtained with an accuracy better than fourteen significant digits. B-splines posses the advantages of completeness and linear independence [31, 32]. Building on these advantages, the developed C-BSBF method explicitly incorporated the interelectronic coordinate r_{12} , allowing it to simultaneously describe short-range electron-electron cusps and long-range asymptotic behavior within a unified basis, thus eliminating the nonlinear-parameter optimization over different radial sectors required in Hylleraas calculations [21].

In this work, the C-BSBF method is extended to compute $1snp\ ^3P_J$ fine-structure intervals of high Rydberg states in $^4{\rm He}$, enabling direct comparison of ab initio results with experimental data. The leading relativistic corrections with nuclear recoil, the anomalous magnetic moment, and singlet-triplet mixing effects are taken into account. Ab initio results are presented for n=24-37, while data for n=45-51 obtained by the 1/n asymptotic expansion are also reported. The inverse fine-structure constant, the electron mass, the nuclear mass of $^4{\rm He}$, and the Rydberg frequency are taken as $\alpha^{-1}=137.035\,999\,177(21)$, $m_e=1,\ M_0=7\,294.299\,541\,71(17)\,m_e$, and $cR_y=3.289\,841\,960\,250\,0(36)\times 10^9$ MHz [33], respectively.

II. THEORETICAL METHOD

Within the nonrelativistic quantum electrodynamics framework, the fine structure splittings of the $n\,^3P_J$ states are obtained by first solving the nonrelativistic Schrödinger equation to determine unperturbed (zerothorder) energies and wave functions. The fine-structure effects are then introduced perturbatively through the Breit-Pauli Hamiltonian [18, 34]. The fine-structure energy-level diagram of the higher Rydberg states $n\,^3P_J\,(J=0,1,2)$ with $n=24,\,27,\,34,\,35,\,36,\,$ and 37 in 4 He is displayed in Fig. 1.

The nonrelativistic Hamiltonian of $^4\mathrm{He}$ in atomic units takes the form

$$H = \frac{p_1^2 + p_2^2}{2\mu_e} + \frac{\mathbf{p}_1 \cdot \mathbf{p}_2}{M_0} - \frac{Z}{r_1} - \frac{Z}{r_2} + \frac{1}{r_{12}},\tag{1}$$

where r_i is the coordinate of the *i*-th electron to the nucleus, $r_{12} = |\mathbf{r}_1 - \mathbf{r}_2|$ is the interelectronic coordinate, M_0 is the nuclear mass of ⁴He, $\mu_e = m_e M_0/(m_e + M_0)$ is the reduced electron mass, and the nuclear charge Z = 2. The $\mathbf{p}_1 \cdot \mathbf{p}_2/M_0$ term is the mass-polarization contribution due to nuclear motion in the center-of-mass frame.

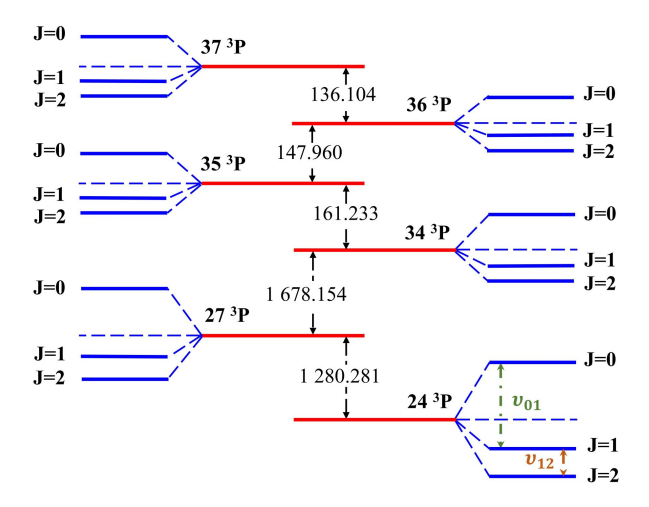


FIG. 1. Fine-structure energy levels (not drawn to scale) for the $n^3 P_J (J=0,1,2)$ states of ⁴He, in GHz.

The two-electron wave functions are expanded in C-BSBFs [28],

$$\phi_{ij,c,\ell_1\ell_2} = \mathcal{A} \left[r_{12}^c B_i^k(r_1) B_i^k(r_2) \mathcal{Y}_{\ell_1\ell_2}^{LM}(\hat{\mathbf{r}}_1, \hat{\mathbf{r}}_2) \right], \quad (2)$$

where \mathcal{A} antisymmetrizes the electrons, c=0 and 1, N is the number of B-splines confined in a cavity of radius R_0 , $B_i^k(r)$ is the i-th B-spline of order k [31], and $\mathcal{Y}_{\ell_1\ell_2}^{LM}$ are coupled spherical harmonics [35, 36]. Orbital angular momenta satisfy $\ell_1, \ell_2 \leq \ell_{\max}$.

The leading contribution to the fine-structure splittings originates from the spin-dependent Breit-Pauli interaction [34] of order $m\alpha^4$, since the spin-independent part contributes equally to all fine structure levels. The effective spin-dependent Breit-Pauli Hamiltonian can be expressed as

$$H_{\rm fs}^{(4)} = H_{\rm so} + H_{\rm soo} + H_{\rm ss} + \Delta,$$
 (3)

with

$$H_{\text{so}} = \frac{Z\alpha^{2}}{2} \left[\frac{\mathbf{r}_{1}}{r_{1}^{3}} \times \mathbf{p}_{1} \cdot \mathbf{s}_{1} + \frac{\mathbf{r}_{2}}{r_{2}^{3}} \times \mathbf{p}_{2} \cdot \mathbf{s}_{2} \right],$$

$$H_{\text{soo}} = \frac{\alpha^{2}}{2r_{12}^{3}} \left[\mathbf{r}_{12} \times \mathbf{p}_{2} \cdot (2\mathbf{s}_{1} + \mathbf{s}_{2}) - \mathbf{r}_{12} \times \mathbf{p}_{1} \cdot (2\mathbf{s}_{2} + \mathbf{s}_{1}) \right],$$

$$H_{\text{ss}} = \alpha^{2} \left[\frac{\mathbf{s}_{1} \cdot \mathbf{s}_{2}}{r_{12}^{3}} - \frac{3(\mathbf{s}_{1} \cdot \mathbf{r}_{12})(\mathbf{s}_{2} \cdot \mathbf{r}_{12})}{r_{12}^{5}} \right],$$

$$\Delta_{\text{so}} = Z\alpha^{2} \left(\frac{\mathbf{r}_{1}}{r_{1}^{3}} \times \mathbf{p}_{2} \cdot \mathbf{s}_{1} + \frac{\mathbf{r}_{2}}{r_{2}^{3}} \times \mathbf{p}_{1} \cdot \mathbf{s}_{2} \right),$$

$$(4)$$

where $H_{\rm so}$ is the spin-orbit interaction, $H_{\rm soo}$ is the spin-other-orbit interaction, $H_{\rm ss}$ is the spin-spin interaction, $\Delta = \frac{m_e}{M_0} \left(\Delta_{\rm so} + 2 H_{\rm so} \right)$ is the Stone term arising in the center-of-mass frame [37, 38], and $\mathbf{s}_{1,2}$ are Pauli spin matrices.

In addition, the contribution of order $m\alpha^5$ arises from the electron anomalous magnetic moment corrections to Breit-Pauli operators, and the effective Hamiltonian has the form of

$$H_{\rm fs}^{(5)} = \frac{\alpha}{\pi} \left[H_{\rm so} + \frac{2}{3} H_{\rm soo} \, \delta_{SS'} + H_{\rm ss} \right],$$
 (5)

where $\delta_{S,S'}$ nulls the single-triplet mixing part of H_{soo} [39–41].

The singlet–triplet mixing correction to the n^3P_1 energy level, induced by the spin-dependent Breit–Pauli operators, is of order $m\alpha^6$. This effect includes both fine- and hyperfine-induced mixing, of which only the fine component is relevant for ⁴He. For higher Rydberg states (larger n), the energy interval between the n^3P_1 and n^4P_1 levels becomes progressively smaller; consequently singlet–triplet mixing grows in significance and must be evaluated with high accuracy. The singlet–triplet contribution is obtained by exact diagonalization of an effective 2×2 Hamiltonian [18, 42, 43], where the mixing correction $\Delta_{\rm mix}$ is defined as the difference between the eigenvalue and the corresponding diagonal element:

$$H_{\text{eff}} = \begin{pmatrix} E_{\text{dia}}(n^3 P_1) & E_{\text{off}} \\ E_{\text{off}} & E_{\text{dia}}(n^1 P_1) \end{pmatrix}, \tag{6}$$

where $E_{\text{dia}}(n^3P_1)$ and $E_{\text{dia}}(n^1P_1)$ correspond to the energies of the triplet and singlet states, respectively, and E_{off} denotes the off-diagonal matrix element responsible for fine mixing, which can be expressed as

$$E_{\text{off}} = \langle n^3 P_1 | H_{\text{mix}} | n^1 P_1 \rangle$$

= $\langle n^1 P_1 | H_{\text{mix}} | n^3 P_1 \rangle$, (7)

here

$$H_{\text{mix}} = H_{\text{so}} + H_{\text{soo}}. \tag{8}$$

In the $|LSJM_J\rangle$ basis, the coupled state can be expressed as

$$|LSJM_{J}\rangle = \sum_{M_{L}M_{S}} |LSM_{L}M_{S}\rangle\langle LSM_{L}M_{S}|LSJM_{J}\rangle, \tag{9}$$

where $|LSM_LM_S\rangle$ denotes the uncoupled LS basis state, in which the orbital angular momentum **L** and total spin **S** are separately quantized before coupling to the total angular momentum $\mathbf{J} = \mathbf{L} + \mathbf{S}$. In this representation, the expectation value of a spin-dependent operator \hat{X} factorizes as

$$\langle \hat{X} \rangle_J = \Lambda(J) \langle \hat{X} \rangle,$$
 (10)

where $\langle \hat{X} \rangle$ denotes the expectation value evaluated in the uncoupled LS basis. The angular-momentum coupling coefficients are given by $\Lambda_J = \{-1/3, -1/6, 1/6\}$ for $H_{\rm so}$ and $H_{\rm soo}$, and $\{1/3, -1/6, 1/30\}$ for $H_{\rm ss}$ at J=0,1,2, respectively.

The fine-structure splittings follow as

$$\nu_{01} = -\frac{1}{6} \left[\langle H_{\rm so} \rangle + \langle H_{\rm soo} \rangle + \langle \Delta \rangle \right] + \frac{1}{2} \langle H_{\rm ss} \rangle$$

$$-\frac{1}{6} \left[\frac{\alpha}{\pi} \langle H_{\rm so} \rangle + \frac{2\alpha}{3\pi} \langle H_{\rm soo} \rangle \right] + \frac{\alpha}{2\pi} \langle H_{\rm ss} \rangle$$

$$-\Delta_{\rm mix},$$

$$\nu_{12} = -\frac{1}{3} \left[\langle H_{\rm so} \rangle + \langle H_{\rm soo} \rangle + \langle \Delta \rangle \right] - \frac{1}{5} \langle H_{\rm ss} \rangle,$$

$$-\frac{1}{3} \left[\frac{\alpha}{\pi} \langle H_{\rm so} \rangle + \frac{2\alpha}{3\pi} \langle H_{\rm soo} \rangle \right] - \frac{\alpha}{5\pi} \langle H_{\rm ss} \rangle$$

$$+\Delta_{\rm mix}.$$
(11)

In practice, one evaluates the combined interval $\nu_{02} = \nu_{01} + \nu_{12}$, for which singlet–triplet mixing cancels exactly [44], whereas this mixing has a significant effect on the individual intervals ν_{01} and ν_{12} .

III. RESULTS AND DISCUSSIONS

In our previous work [30], a cavity radius of $R_0 = 2400$ a.u. allowed accurate calculations of nonrelativistic energies up to n = 27. In the present study, the extension to higher Rydberg states inevitably requires a larger cavity radius, as the electronic radial distribution at $n \sim 37$ spans much larger distances. Through semi-empirical parameters adjusting, the cavity radius is currently chosen to be $R_0 = 4000$ a.u.. Increasing the cavity size, however, imposes more stringent demands on numerical integration. To ensure computed accuracy and stability across the entire radial interval, numerically improved Laplace expansions and an efficient adaptive integration scheme were employed.

Calculations were performed using B-splines of sizes $N=80,\,90,\,$ and 100 for $\ell_{\rm max}=4,\,$ while an additional calculation with N=100 and $\ell_{\rm max}=5$ was carried out to evaluate the influence of the $\ell_{\rm max}$ truncation. The corresponding basis dimensions reached up to 80 000 and 100 000 for $\ell_{\rm max}=4$ and 5, respectively, and full diagonalization was performed using a self-developed quadruple-precision parallel program. The convergence uncertainty was defined as the larger of the two sources of numerical deviation: (i) the maximum difference between the extrapolated value and the results from the three largest basis sets $(N=80,\,90,\,$ and 100 at $\ell_{\rm max}=4),\,$ and (ii) the change in the result when $\ell_{\rm max}$ was increased from 4 to 5

At first, energies of the n^3P series were calculated for both infinite nuclear mass of helium and $^4{\rm He}$. For the case of n=24 with infinite nuclear mass, the present C-BSBF calculation yields an energy of $-2.000\,873\,014\,566\,616\,659(2)$ a.u., which agrees with the Hylleraas result [21] to eighteen significant digits, confirming the high accuracy of the present approach. Non-relativistic energies of the n^3P states with n=24-37 for $^4{\rm He}$ are listed in Table I. The calculated energies are

TABLE I. Nonrelativistic energies (in a.u.) of the n^3P states and expectation values (in $10^{-5}\alpha^2$ a.u.) of spin-dependent Breit operators for the n^3P_1 states of 4 He (n=24–37). For each principal quantum number, the first line presents the current results for 4 He, the second line lists Hylleraas reference data from Ref. [25]. The calculations adopt node parameter $\tau=0.00228$, spline order k=15, $\ell_{\rm max}=4$, and box size $R_0=4000$ a.u.. The notation $\langle X \rangle_1^+$ indicates the expectation value including finite nuclear mass effects. The numbers in parentheses are the convergence uncertainties.

\overline{n}	⁴ He	$\langle H_{\rm so} \rangle_1^+$	$\langle H_{\rm soo} \rangle_1^+$	$\langle H_{\rm ss} \rangle_1^+$	$\langle \Delta_{ m so} angle_1^+$
24	-2.000598750318682937(1)	-1.8548785388401(2)	2.67567279(1)	-1.08783865(1)	5.4281800493824(4)
	` '	-1.854878538847(9)	2.675672783442(7)	-1.0878386497847(15)	5.428 180 049 6(18)
25	-2.000530131464088097(6)	-1.6405152987431(4)	2.366 412 90(1)	-0.96207075(1)	4.800 863 560 988(1)
	• •	-1.640515298741(9)	2.366 412 898 439(9)	-0.9620707445341(32)	4.800 863 561 0(5)
26	-2.00046929688728100(2)	-1.4579506826781(1)	2.10303555(1)	-0.85496789(1)	4.2666025169822(2)
	` ,	-1.457950682662(19)	2.103035544451(24)	-0.854967883837(6)	4.266 602 517 38(20)
27	-2.00041511219560993(4)	-1.301500491618(2)	1.87733753(1)	-0.76319182(1)	3.808 762 819 451(6)
		-1.3015004916374(16)	1.877337528619(9)	-0.7631918217910(8)	3.808 762 822 8(9)
28	-2.00036664235361461(8)	-1.166657507730(4)	1.682 814 55(1)	-0.68409594(1)	3.41415462681(1)
	` '	-1.166657507732(7)	1.682814549259(22)	-0.684095937963(8)	3.4141546252(4)
29	-2.0003231110726965(2)	-1.049816704402(8)	1.514 264 48(1)	-0.61556366(1)	3.07222823126(2)
		-1.049816704323(11)	1.514 264 474 503 4(27)-0.6155636618175(11)	3.072 228 04(8)
30	-2.0002838695343599(8)	-0.94807139766(2)	1.36749306(1)	-0.55588864(1)	2.774 477 530 87(6)
		-0.948071397669(10)	1.36749306154(7)	-0.555888638049(24)	2.774477524(11)
31	-2.000248372073557(2)	-0.85906038247(6)	1.23909330(1)	-0.50368489(1)	2.5139926983(2)
		-0.8590603824702(30)	1.239 093 296 767 2(37)-0.5036848836715(11)	2.51399270013(9)
32	-2.000216157106699(7)	-0.7808521449(2)	1.12627827(1)	-0.45781875(1)	2.2851213454(6)
		-0.7808521448902(37)	1.126278262651(7)	-0.457818747772(7)	2.28512124(5)
33	-2.00018683205030(2)	-0.7118563330(6)	1.02675336(1)	-0.41735690(1)	2.083209455(2)
		-0.711856332881(10)	1.0267533597564(15)-0.4173568985808(5)	2.083 209 31(11)
34	-2.00016006130370(7)	-0.650755474(2)	0.93861776(1)	-0.38152621(1)	1.904401561(6)
		-0.65075547371(16)	0.9386177563(15)	-0.3815262120(8)	1.9044021(4)
35	-2.0001355566046(2)	-0.596451875(6)	0.86028775(1)	-0.34968258(1)	1.74548536(2)
		-0.5964518707(25)	0.8602877531(6)	-0.34968258377233(6)	1.745482(4)
36	-2.0001130692365(7)	-0.54802601(2)	0.79043673(3)	-0.32128649(1)	1.603 769 93(6)
37	-2.000092383692(8)	-0.5047037(8)	0.727948(1)	-0.2958838(6)	1.476 989(2)

found to have converged to at least 13 significant digits. All these states were obtained from a single diagonalization without any state-dependent parameter optimization, demonstrating the numerical stability and computational efficiency of the C-BSBF method in describing higher Rydberg states. In addition, we analyzed the effect of the uncertainty in the nuclear mass of 4 He, M_0 [33], on the nonrelativistic energies. This uncertainty leads to variations at the 14th–15th decimal places, which do not affect the fine-structure splittings calculated in the following sections and are therefore neglected in the present work.

Using Eq. (10), the contributions of the spin-dependent operators to the different n^3P_J states are obtained. The results for the n^3P_1 state are listed in Table I, where the notation $\langle X \rangle_1^+$ denotes the expectation value including the finite nuclear mass correction. These values are required for evaluating the $m\alpha^4$ - and $m\alpha^5$ -order contributions to the fine-structure splittings. The numerical accuracy of these values ensures a precision at the kHz level in the fine-structure splitting calculations. Table I also compares the present C-BSBF results with the Hylleraas data [25], where the latter were obtained by combining the infinite-nuclear-mass matrix elements with the corresponding mass-polarization corrections. The two sets of matrix elements differ only beyond the sixth significant figure, resulting in differences in the fine-structure split-

tings below 10 Hz—well below the current experimental accuracy and therefore negligible.

The $m\alpha^4$ - and $m\alpha^5$ -order contributions to the finestructure intervals ν_{12} and ν_{02} in ⁴He, obtained using the C-BSBF method, are summarized in Table II. For the J=1 level, the singlet-triplet mixing term contributes at order $m\alpha^6$, while it has no effect for J=0 or J=2; the corresponding correction to ν_{12} , denoted as Δ_{mix} , is also listed in Table II. To date, complete calculations of the fine-structure splittings including all terms up to order $m\alpha^7$ have been performed only for the 2^3P_J and $3^{3}P_{J}$ states of helium [6, 45–47]. For higher Rydberg states, the present work estimated the $m\alpha^6$ contributions by extrapolating the $2^{3}P_{J}$ results [6] according to a $1/n^{3}$ scaling, following the approach adopted in previous studies [21]. As summarized in Table II, the uncertainties of the calculated fine-structure splittings for ⁴He with principal quantum numbers n = 24-37 are all below 5 kHz, indicating the high numerical precision achieved in the present C-BSBF computations. The overall uncertainty of the fine-structure splittings is dominated by the extrapolation of the $m\alpha^6$ contribution.

As shown in Table II, comparisons are made among the present C-BSBF results, the Hylleraas calculations [25], and the QDT predictions. The fine-structure splittings for n=24–35 obtained with the Hylleraas basis were inferred from the calculated energies of the $n\,^3P_{0,1,2}$ states

TABLE II. Breakdown of the fine-structure intervals ν_{12} and ν_{02} (in MHz) of the n^3P_J states of ⁴He for n=24–37. The entries are labeled as follows: " $m\alpha^4$ " is the relativistic correction including finite nuclear mass effects; " $m\alpha^5$ " is anomalous magnetic moment correction; " Δ_{mix} " is the singlet-triplet mixing term; "Total" is the total fine-structure splittings. Present results are compared with Hylleraas values [25], QDT, and experimental data [15].

n	$m lpha^4$	$m lpha^5$	$\Delta_{ m mix}$	Total	Hylleraas [25]	QDT	Exp. [15]
			$ u_{12}$				
24	1.179556	-0.011783	-0.002266	1.1655(38)	1.1661(16)	1.1656	
25	1.043168	-0.010421	-0.002005	1.0307(33)	1.0315(16)	1.0308	
26	0.927023	-0.009262	-0.001782	0.9160(30)	0.9168(14)	0.9160	
27	0.827501	-0.008268	-0.001591	0.8176(26)	0.8185(14)	0.8177	
28	0.741732	-0.007411	-0.001426	0.7329(24)	0.7339(14)	0.7329	
29	0.667419	-0.006669	-0.001283	0.6595(21)	0.6605(14)	0.6595	
30	0.602711	-0.006023	-0.001159	0.5955(19)	0.5966(14)	0.5955	
31	0.546106	-0.005457	-0.001051	0.5396(17)	0.5408(13)	0.5396	
32	0.496373	-0.004960	-0.000955	0.4905(16)	0.4917(13)	0.4905	
33	0.452500	-0.004522	-0.000871	0.4471(14)	0.4483(13)	0.4471	
34	0.413650	-0.004134	-0.000796	0.4087(13)	0.4100(13)	0.4087	0.397
35	0.379123	-0.003789	-0.000730	0.3746(12)	0.3759(13)	0.3746	0.366
36	0.348334	-0.003481	-0.000670	0.3442(11)		0.3442	0.340
37	0.320791	-0.003206	-0.000617	0.3170(10)		0.3170	
			$ u_{02}$				
24	15.490868	0.014205		15.5051(47)	15.5013(16)	15.5051	
25	13.699902	0.012562		13.7125(42)	13.7092(16)	13.7125	
26	12.174736	0.011163		12.1859(37)	12.1831(14)	12.1859	
27	10.867829	0.009964		10.8778(33)	10.8753(14)	10.8778	
28	9.741493	0.008931		9.7504(30)	9.7484(14)	9.7504	
29	8.765586	0.008036		8.7736(27)	8.7718(14)	8.7736	
30	7.915809	0.007257		7.9231(24)	7.9215(14)	7.9231	
31	7.172425	0.006575		7.1790(22)	7.1777(13)	7.1790	
32	6.519290	0.005976		6.5253(20)	6.5241(13)	6.5253	
33	5.943113	0.005448		5.9486(18)	5.9476(13)	5.9486	
34	5.432884	0.004980		5.4379(17)	5.4371(13)	5.4379	5.387
35	4.979431	0.004564		4.9840(15)	4.9833(13)	4.9840	5.014
36	4.575072	0.004194		4.5793(14)	, ,	4.5793	4.643
37	4.21334	0.003862		4.2172(13)		4.2172	

reported in Ref. [25]. The uncertainties were determined as the square root of the sum of the squared uncertainties of the two corresponding energy levels. Since the radiative $m\alpha^6$ corrections were included in those calculations, the dominant source of uncertainty originates from the nonradiative $m\alpha^6$ contributions. QDT values listed in Table II for n = 24-37 were obtained by using Drake's quantum defect parameters [48]. QDT provides an alternative method for determining energies and fine-structure splittings of higher Rydberg states, particularly when ab initio calculations become increasingly demanding due to electron correlation and core potential complexity [49, 50]. As can be seen from the table, the fine-structure splittings obtained with the C-BSBFs and Hylleraas basis are consistent with each other within uncertainties, and also agree well with the QDT predictions. This cross-validation between two ab initio approaches, together with the agreement with QDT, provides an evidence for the reliability of the present C-BSBF computations.

For n = 34-36, the present C-BSBF results enable a

direct comparison between ab initio calculations and experimental measurements. The measured values of both ν_{12} and ν_{02} obtained by microwave spectroscopy [15] are listed in the last column of Table II. For ν_{12} and ν_{02} , the relative deviations of the present calculations from the experimental values are below 3\% and 1.5\%, respectively. These deviations exceed the relative uncertainties of the experimental measurements, which are at the level of a few thousandths. However, the reported experimental uncertainties of 15-40 kHz do not include systematic contributions. A large deviation occurs at n = 34, where the measured ν_{02} interval differs from the quantum-defect prediction by about 4.2σ [15], while the present C-BSBF and Hylleraas [25] results remain in excellent agreement with QDT, confirming the reliability of the theoretical framework. Better control of stray electric and magnetic fields is expected to reduce systematic uncertainties in the measured fine-structure intervals to the order of 1 kHz [15], allowing a more stringent comparison with the ab initio theoretical calculations.

Having calculated the expectation values of the spin-

TABLE III. 1/n asymptotic expansion coefficients in Eq. (12) for the spin-dependent Breit operators and singlet-triplet mixing in the n^3P_1 states, and for the fine-structure splittings of the n^3P_J states in 4 He.

Terms	c_0	c_1	c_2
$\langle H_{\rm so} \rangle_1^+$	-0.254231	-0.052224	-0.006287
$\langle H_{\rm soo} \rangle_1^+$	0.366653	0.075264	0.055483
$\langle H_{\rm ss} \rangle_1^+$	-0.149004	-0.030530	-0.061548
$\langle \Delta_{\rm so} \rangle_1^+$	0.743997	0.152890	0.013743
$\Delta_{ m mix}$	-31.196028	-2.609676	-14.351107
ν_{12}	1.596051×10^4	3.277532×10^3	8.577158×10^3
ν_{02}	2.123714×10^5	4.351912×10^4	9.069520×10^4

dependent operators and the singlet—triplet mixing term, as well as the fine-structure splittings for a series of $n\,^3P_J$ states, we can now analyze their n dependence. The numerical results listed in Tables I and II were fitted to a 1/n asymptotic expansion of the following form:

$$\langle \hat{X} \rangle = \frac{1}{n^3} \sum_{i=0}^2 \frac{c_i}{n^i} \,. \tag{12}$$

The obtained coefficients c_i are presented in Table III. Using the parameters c_0 , c_1 , and c_2 , the fitted values of ν_{12} and ν_{02} for n=37 are 0.316 97 and 4.217 20 MHz, respectively. These fitted values are in good agreement with the present ab initio fine-structure splittings, demonstrating the reliability of the 1/n asymptotic expansion. Using this expansion, both the contributions from the spin-dependent operators and the singlet-triplet mixing term, as well as the fine-structure splittings for higher Rydberg states, can be predicted.

TABLE IV. Comparison between theoretical and experimental values of the fine-structure interval $\nu_{(0,\overline{12})}$ (in kHz) for the $n\,^3P_J\,(n=45-51)$ states in $^4{\rm He}$.

	- ,		
\overline{n}	Present	QDT	Exp. [15]
45	2275.656	2275.66	2 243
46	2130.218	2130.22	2150
47	1996.914	1996.92	1971
48	1874.505	1874.51	1817
49	1761.899	1761.90	1813
50	1658.136	1658.14	1646
51	1562.363	1562.36	1476

Using Eq. (12) and the fitted coefficients given in Table III, the calculated fine-structure splittings for n=45-51 are presented in Table IV. To facilitate comparison with the experimental measurements [15], the weighted-average values $\nu_{0,\overline{12}}$ are reported, since the fine-structure intervals decrease as n^{-3} , making ν_{12} increasingly difficult to resolve for higher n in the experiment. The QDT predictions listed in Table IV are also weight-averaged. As shown in the table, the present fitted results are in excellent agreement with the QDT values, with discrep-

ancies below 0.01 kHz across the entire range, demonstrating that the fitted parameters reliably describe the fine structure of the $n\,^3P$ higher Rydberg series in 4 He. The relative deviations of the fitted results from the measurements [15] are within 6%. This discrepancy may be attributed to unresolved theoretical effects and limitations in the experimental precision, highlighting the need for further refinement in both theory and measurement.

IV. CONCLUSION

In summary, we have extended the correlated B-spline basis function (C-BSBF) method to compute the fine-structure splittings of high Rydberg states in ⁴He. The method accurately incorporates both electron–electron correlation and long-range asymptotic behavior within a unified basis, allowing stable and precise ab initio calculations for large-n states. Corrections of orders $m\alpha^4$ and $m\alpha^5$, as well as singlet–triplet mixing contributions of order $m\alpha^6$ were evaluated explicitly, while the spin-dependent $m\alpha^6$ contributions were estimated using a $1/n^3$ scaling extrapolation from low-lying states.

For principal quantum numbers n=24–37, the present calculations achieve kHz-level accuracy in the fine-structure intervals ν_{12} and ν_{02} . The results show excellent agreement with both Hylleraas-basis ab initio data and quantum-defect-theory (QDT) predictions, demonstrating the reliability of the C-BSBF approach for describing highly excited two-electron systems. Based on these high-precision results, the fine-structure splittings for n=45–51 were further obtained through 1/n-asymptotic fitting, yielding values that reproduce QDT predictions within 0.01 kHz and agree with experimental measurements within 6%.

The demonstrated capability of the C-BSBF method to achieve kHz-level precision for helium Rydberg fine structures provides a solid foundation for future inclusion of complete $m\alpha^6$ and $m\alpha^7$ QED corrections. Moreover, detailed comparisons between high-accuracy theory and precision spectroscopy of high-n Rydberg states will enable stringent tests of QED and may serve as a sensitive probe for subtle or previously unaccounted physical effects in two-electron systems.

ACKNOWLEDGMENTS

This work is supported by the National Natural Science Foundation of China under Grants No. 12274417, No. 12274423, No. 12393821, No. 12204412, and No. 12174402, by the Chinese Academy of Sciences Project for Young Scientists in Basic Research under Grant No. YSBR-055, and by the Pioneer Research Project for Basic and Interdisciplinary Frontiers of Chinese Academy of Sciences under Grants No. XDB0920101 and XDB0920100. Theoretical calculations were done on the APM-Theoretical Computing Cluster(APM-TCC).

V. APPENDIX

This Appendix presents the fine-structure splittings of ${}^{4}\text{He }n{}^{3}P_{J}$ states for principal quantum numbers 11 \leq $n \leq 37$. In addition to the present calculations, Table V

- also includes results from quantum defect theory (QDT) and recent high-accuracy calculations by Drake et al. [25]. The uncertainties of the latter are defined as the square root of the sum of the squared uncertainties of the corresponding level energies [25]. The present results are in agreement with those of Drake et al. [25] within uncertainties.
- C. Schwartz, Fine structure of helium, Phys. Rev. 134, A1181 (1964).
- [2] X. Zheng, Y. R. Sun, J.-J. Chen, W. Jiang, K. Pachucki, and S.-M. Hu, Laser spectroscopy of the fine-structure splitting in the 2³P_J levels of ⁴He, Phys. Rev. Lett. 118, 063001 (2017).
- [3] K. Pachucki, V. Patkóš, and V. A. Yerokhin, Testing fundamental interactions on the helium atom, Phys. Rev. A 95, 062510 (2017).
- [4] K. Kato, T. D. G. Skinner, and E. A. Hessels, Ultrahigh-precision measurement of the n = 2 triplet P fine structure of atomic helium using frequency-offset separated oscillatory fields, Phys. Rev. Lett. 121, 143002 (2018).
- [5] F. Heydarizadmotlagh, T. D. G. Skinner, K. Kato, M. C. George, and E. A. Hessels, Precision measurement of the n = 2 triplet P J = 1 to J = 0 fine structure of atomic helium using frequency-offset separated oscillatory fields, Phys. Rev. Lett. 132, 163001 (2024).
- [6] K. Pachucki and V. A. Yerokhin, Fine structure of heliumlike ions and determination of the fine structure constant, Phys. Rev. Lett. 104, 070403 (2010).
- [7] K. Pachucki, Improved theory of helium fine structure, Phys. Rev. Lett. 97, 013002 (2006).
- [8] E. A. Hessels, P. W. Arcuni, F. J. Deck, and S. R. Lundeen, Microwave spectroscopy of high-L, n=10 Rydberg states of helium, Phys. Rev. A 46, 2622 (1992).
- [9] N. E. Claytor, E. A. Hessels, and S. R. Lundeen, Fastbeam measurements of the 10D-10F fine-structure intervals in helium, Phys. Rev. A 52, 165 (1995).
- [10] C. H. Storry, N. E. Rothery, and E. A. Hessels, Precision separated-oscillatory-field measurement of the n = 10⁺F₃ ⁺G₄ interval in helium: A precision test of long-range relativistic, radiative, and retardation effects, Phys. Rev. Lett. **75**, 3249 (1995).
- [11] G. D. Stevens and S. R. Lundeen, Measurements of G-H and H-I fine-structure intervals in n=7, 9, and 10 helium Rydberg states, Phys. Rev. A **60**, 4379 (1999).
- [12] P. Rabl, D. DeMille, J. M. Doyle, M. D. Lukin, R. J. Schoelkopf, and P. Zoller, Hybrid quantum processors: Molecular ensembles as quantum memory for solid state circuits. Phys. Rev. Lett. 97, 033003 (2006).
- [13] S. D. Hogan, J. A. Agner, F. Merkt, T. Thiele, S. Filipp, and A. Wallraff, *Driving Rydberg-Rydberg transitions from a coplanar microwave waveguide*, Phys. Rev. Lett. 108, 063004 (2012).
- [14] V. Zhelyazkova and S. D. Hogan, Electrically tuned Förster resonances in collisions of NH₃ with Rydberg He atoms, Phys. Rev. A 95, 042710 (2017).
- [15] A. Deller and S. D. Hogan, Microwave spectroscopy of the 1snp ³P_J fine structure of high Rydberg states in ⁴He, Phys. Rev. A 97, 012505 (2018).

- [16] G. W. F. Drake, High precision theory of atomic helium, Phys. Scr. 1999, 83 (1999).
- [17] G. W. F. Drake, Quantum defect theory and analysis of high-precision helium term energies, vol. 32 (Academic Press, 1993).
- [18] G. W. F. Drake and Z.-C. Yan, Energies and relativistic corrections for the Rydberg states of helium: Variational results and asymptotic analysis, Phys. Rev. A 46, 2378 (1992).
- [19] G. W. F. Drake and W. C. Martin, Ionization energies and quantum electrodynamic effects in the lower 1sns and 1snp levels of neutral helium (⁴He I), Can. J. Phys. 76, 679 (1998).
- [20] D. T. Aznabaev, A. K. Bekbaev, and V. I. Korobov, Nonrelativistic energy levels of helium atoms, Phys. Rev. A 98, 012510 (2018).
- [21] A. T. Bondy, G. W. F. Drake, C. McLeod, E. M. R. Petrimoulx, X.-Q. Qi, and Z.-X. Zhong, Theory for the Rydberg states of helium: Comparison with experiment for the 1s24p ¹P₁ state (n = 24), Phys. Rev. A 111, L010803 (2025).
- [22] G. Clausen, P. Jansen, S. Scheidegger, J. A. Agner, H. Schmutz, and F. Merkt, *Ionization energy of the metastable 2* ¹S₀ state of ⁴He from Rydberg-series extrapolation, Phys. Rev. Lett. **127**, 093001 (2021).
- [23] G. Clausen, K. Gamlin, J. A. Agner, H. Schmutz, and F. Merkt, Metrology in a two-electron atom: The ionization energy of metastable triplet helium 2³S₁, Phys. Rev. A 111, 012817 (2025).
- [24] G. Clausen and F. Merkt, Ionization energy of metastable ³He (2 ³S₁) and the alpha- and helion-particle charge-radius difference from precision spectroscopy of the np Rydberg series, Phys. Rev. Lett. **134**, 223001 (2025).
- [25] G. W. F. Drake, A. T. Bondy, O. P. Hallett, and B. C. Najem, Theory for the Rydberg states of helium: Results for $2 \le n \le 35$ and comparison with experiment for the singlet and triplet P-states, arXiv:2510.17495 (2025).
- [26] S. J. Yang, X. S. Mei, T. Y. Shi, and H. X. Qiao, Application of the Hylleraas-B-spline basis set: Static dipole polarizabilities of helium, Phys. Rev. A 95, 062505 (2017).
- [27] S. J. Yang, Y. B. Tang, Y. H. Zhao, T. Y. Shi, and H. X. Qiao, Application of the Hylleraas-B-spline basis set: Nonrelativistic Bethe logarithm of helium, Phys. Rev. A 100, 042509 (2019).
- [28] H. Fang, Y. H. Zhang, P. P. Zhang, and T. Y. Shi, Application of the correlated B-spline basis functions to the leading relativistic and QED corrections of helium, Phys. Rev. A 108, 062818 (2023).
- [29] H. Fang, Y. H. Zhang, L. Y. Tang, and T. Y. Shi, Sub-parts-per-million theoretical calculations of dipole polarizabilities for helium n^{1,3}S (n = 1 to 7) states using correlated B-spline basis functions, Phys. Rev. A 110, 062823

TABLE V. Comparison of fine-structure intervals between the n^3P_J levels in ⁴He obtained from different methods (in MHz).

\overline{n}	$ u_{12}$	$\nu_{12} [25]$	QDT	$ u_{02}$	$ u_{02} \ [25]$	QDT
11	12.268(39)	12.260(18)	12.44	163.094(49)	163.047(18)	163.27
12	9.429(30)	9.422(14)	9.50	125.364(38)	125.328(14)	125.43
13	7.402(24)	7.398(11)	7.430	98.432(30)	98.404(11)	98.460
14	5.918(19)	5.914(8)	5.9299	78.696(24)	78.674(8)	78.7085
15	4.805(15)	4.802(7)	4.8108	63.904(19)	63.886(7)	63.9096
16	3.955(13)	3.9530(52)	3.9576	52.599(16)	52.5843(52)	52.6019
17	3.294(11)	3.2926(41)	3.2954	43.811(13)	43.7991(41)	43.8128
18	2.7725(89)	2.7717(33)	2.7733	36.877(11)	36.8673(33)	36.8782
19	2.3556(75)	2.3551(27)	2.3560	31.3330(95)	31.3245(27)	31.3335
20	2.0182(65)	2.0181(21)	2.0185	26.8468(81)	26.8396(21)	26.8470
21	1.7424(56)	1.7419(17)	1.7425	23.1778(70)	23.1717(17)	23.1779
22	1.5146(49)	1.5149(17)	1.5147	20.1481(61)	20.1429(17)	20.1482
23	1.3248(43)	1.3253(16)	1.3249	17.6243(53)	17.6198(16)	17.6244
24	1.1655(38)	1.1661(16)	1.1656	15.5051(47)	15.5013(16)	15.5051
25	1.0307(33)	1.0315(16)	1.0308	13.7125(42)	13.7092(16)	13.7125
26	0.9160(30)	0.9168(14)	0.9160	12.1859(37)	12.1831(14)	12.1859
27	0.8176(26)	0.8185(14)	0.8177	10.8778(33)	10.8753(14)	10.8778
28	0.7329(24)	0.7339(14)	0.7329	9.7504(30)	9.7484(14)	9.7504
29	0.6595(21)	0.6605(14)	0.6595	8.7736(27)	8.7718(14)	8.7736
30	0.5955(19)	0.5966(14)	0.5955	7.9231(24)	7.9215(14)	7.9231
31	0.5396(17)	0.5408(13)	0.5396	7.1790(22)	7.1777(13)	7.1790
32	0.4905(16)	0.4917(13)	0.4905	6.5253(20)	6.5241(13)	6.5253
33	0.4471(14)	0.4483(13)	0.4471	5.9486(18)	5.9476(13)	5.9486
34	0.4087(13)	0.4100(13)	0.4087	5.4379(17)	5.4371(13)	5.4379
35	0.3746(12)	0.3759(13)	0.3746	4.9840(15)	4.9833(13)	4.9840
36	0.3442(11)		0.3442	4.5793(14)		4.5793
37	0.3170(10)		0.3170	4.2172(13)		4.2172

(2024).

- [30] J. Chi, H. Fang, Y.-H. Zhang, X.-Q. Qi, L.-Y. Tang, and T.-Y. Shi, Accurate nonrelativistic energy calculations for helium 1snp^{1,3}P (n = 2 to 27) states via correlated Bspline basis functions, Atoms 13, 72 (2025).
- [31] H. Bachau, E. Cormier, P. Decleva, J. E. Hansen, and F. Martín, Applications of B-splines in atomic and molecular physics, Rep. Prog. Phys. 64, 1815 (2001).
- [32] C. Froese Fischer, B-splines in variational atomic structure calculations, vol. 55 of Advances In Atomic, Molecular, and Optical Physics (Academic, New York, 2008).
- [33] P. J. Mohr, D. B. Newell, B. N. Taylor, and E. Tiesinga, CODATA recommended values of the fundamental physical constants: 2022, Rev. Mod. Phys. 97, 025002 (2025).
- [34] H. A. Bethe and E. E. Salpeter, Quantum Mechanics of One- and Two-Electron Atoms (Springer Berlin Heidelberg, Berlin, Heidelberg, 1957).
- [35] D. M. Brink and G. R. Satchler, *Angular Momentum* (Oxford University Press, Oxford, New York, 1994).
- [36] G. W. F. Drake, Angular integrals and radial recurrence relations for two-electron matrix elements in Hylleraas coordinates, Phys. Rev. A 18, 820 (1978).
- [37] A. P. Stone, Nuclear and Relativistic Effects in Atomic Spectra, Proc. Phys. Soc. 77, 786 (1961).
- [38] A. P. Stone, Nuclear and Relativistic Effects in Atomic Spectra: II, Proc. Phys. Soc. 81, 868 (1963).
- [39] G. Araki, M. Ohta, and K. Mano, Triplet Intervals of Helium, Phys. Rev. 116, 651 (1959).
- [40] L. Hambro, Second-Order Corrections to the Fine Structure of Helium, Phys. Rev. A 5, 2027 (1972).

- [41] M. L. Lewis and P. H. Serafino, Second-order contributions to the fine structure of helium from all intermediate states, Phys. Rev. A 18, 867 (1978).
- [42] G. W. F. Drake, Unified relativistic theory for $1s2p\ ^3P_1$ $1s^2\ ^1S_0$ and $1s2p\ ^1P_1$ $1s^2\ ^1S_0$ frequencies and transition rates in heliumlike ions, Phys. Rev. A **19**, 1387 (1979).
- [43] G. W. Drake, Theoretical energies for the n = 1 and 2 states of the helium isoelectronic sequence up to Z = 100, Can. J. Phys. 66, 586 (1988).
- [44] K. Pachucki and V. A. Yerokhin, Reexamination of the helium fine structure, Phys. Rev. A 79, 062516 (2009).
- [45] P.-P. Zhang, Z.-X. Zhong, Z.-C. Yan, and T.-Y. Shi, Precision calculation of fine structure in helium and Li⁺, Chin. Phys. B 24, 033101 (2015).
- [46] Z.-C. Yan and G. W. F. Drake, High precision calculation of fine structure splittings in helium and He-like ions, Phys. Rev. Lett. 74, 4791 (1995).
- [47] P. Mueller, L. B. Wang, G. W. F. Drake, K. Bailey, Z. T. Lu, and T. P. O'Connor, Fine structure of the 1s3p ³P_J level in atomic ⁴He: Theory and experiment, Phys. Rev. Lett. 94, 133001 (2005).
- [48] G. W. F. Drake, ed., Springer Handbook of Atomic, Molecular, and Optical Physics, Springer Handbooks (Springer International Publishing, Cham, 2023).
- [49] M. J. Seaton, Quantum defect theory, Rep. Prog. Phys. 46, 167 (1983).
- [50] M. Aymar, C. H. Greene, and E. Luc-Koenig, Multichannel Rydberg spectroscopy of complex atoms, Rev. Mod. Phys. 68, 1015 (1996).